MAGNETIC INDUCTION TOMOGRAPHY SPECTROSCOPY OF LIVING TISSUES: PRINCIPLES AND THEORY

H. Scharfetter*, P. Brunner*, A. Missner*, K. Hollaus* and R. Merwa*

* Institute for Medical Engineering, Graz University of Technology, Graz, Austria
** Institute for Fundamentals and Theory in Electrical Engineering, Graz University of Technology, Graz, Austria

Hermann.scharfetter@tu-graz.at

Abstract: Magnetic Induction Tomography (MIT) is a non-invasive, contact-less method for the reconstruction of changes of the complex electrical conductivity κ in a body. MIT is based on the perturbation of an alternating magnetic field by the object and can be used in all applications of electrical impedance tomography (EIT), e. g. functional lung monitoring and assessment of the tissue fluids. MIT does not require electrodes and works also in the brain where EIT performs very poorly. We present the general framework for MIT-spectroscopy (MITS), a frequency-differential version which exploits the frequency dependence of κ in biological tissues. MITS allows the tissue characterization in the absence of dynamical changes $\Delta\kappa$, e. g. in motionless organs like the brain.

Method

Magnetic induction tomography (MIT) [2] aims at reconstructing the distribution of changes $\Delta\kappa$ of the conductivity $\kappa=\sigma+j\omega\varepsilon\varepsilon_0$ in a target object. The measurement principle is based on determining the perturbation $\mathbf{\Delta B}$ of an alternating magnetic field $\mathbf{B_0}$, which is coupled from an excitation coil (EXC) to the object under investigation. The corresponding voltages ΔV and V_0 induced in a moving receiver coil or a receiver coil array form then the base for the image reconstruction. Possible medical applications are: Detection and monitoring of brain edema, monitoring of lung function, monitoring of wound healing, early detection and classification of stroke etc.

MIT requires the iterative solution of a non-linear inverse eddy current problem. Be

$$\mathbf{y}=\Psi(\boldsymbol{\kappa}) \tag{1}$$

the discretized non-linear forward mapping of the conductivity vector $\boldsymbol{\kappa}$ to the vector of induced voltage $\mathbf{y}$. $\mathbf{y}$ contains $M = a \times b$ entries, a being the number of EXC and b that of receiving coils. The corresponding inverse problem

$$\boldsymbol{\kappa}=\Psi^{-1}(\mathbf{y}) \tag{2}$$

is non-linear, ill-posed and usually underdetermined. The generic approach is the iterative solution of a minimum-norm problem according to:

$$\boldsymbol{\kappa}^* = \arg\min_{\boldsymbol{\kappa}}\left((\Psi(\boldsymbol{\kappa})-\mathbf{y}_m))^T(\Psi(\boldsymbol{\kappa})-\mathbf{y}_m))+\lambda\boldsymbol{\kappa}^T\mathbf{R}^T\mathbf{R}\boldsymbol{\kappa}\right) \tag{3}$$

.

For small perturbations $\mathbf{\Delta\kappa}$ of the vector $\boldsymbol{\kappa}$ of the discretized conductivity the linearization of the problem yields:

$$\Delta\boldsymbol{\kappa}=-(\mathbf{G}^T\mathbf{G}+\lambda\mathbf{R}^T\mathbf{R})^{-1}\mathbf{G}^T\Delta\mathbf{V} \tag{5}$$

with: $\mathbf{\Delta V}$: vector of measured voltage changes in the receiver coils due to $\mathbf{\Delta\kappa}$, $\mathbf{G}$: sensitivity matrix, $\mathbf{R}$: regularization matrix, λ: regularization parameter. The conductivity differences to be reconstructed can be due to dynamic physiological processes (e. g. breathing, pulsations of a vessel) or due to measurements at two different frequencies. The latter case relies on the fact that all biological tissues exhibit a characteristic dependence of the conductivity on the frequency (dispersion). In motionless organs, such as the brain, dynamic imaging is not feasible and only a frequency differential approach can be successful.

Changes of $\boldsymbol{\kappa}$ due to a frequency change Δf can be evaluated at multiple frequencies so as to yield a differential conductivity spectrum $\mathbf{\Delta\kappa}(\Delta f)$. In this case also the Gauss-Newton step (5) can be used, assuming that the conductivity change in the observed frequency interval is small enough. From the literature it is well-known [2,6] that for a given $\mathbf{\Delta\kappa}$ $\mathbf{\Delta V}$ increases with the square of the frequency. Taking the excitation current as a reference, the real part of $\mathbf{\Delta V}$ corresponds to the real part $\mathbf{\Delta\sigma}$ = Re($\mathbf{\Delta\kappa}$). In practice mostly only this real part is evaluated because the imaginary part is usually heavily corrupted by different interferences and systematic errors [6]. Due to the quadratic dependence of the sensitivity on the frequency, the measured voltages must be scaled appropriately. $\mathbf{\Delta V}$ has to be replaced with the scaled version of the real part [6]:

ISSN: 1727-1983

$$\Delta \mathbf{V}(\omega_{ref}, \omega) = \mathrm{Re}\left\{ \mathbf{V}(\omega_{ref}) - \left(\frac{\omega_{ref}}{\omega} \right)^2 \mathbf{V}(\omega) \right\} \quad (6)$$

This formulation relies on the assumption that the morphology of the sensitivity map does not depend on the frequency, which is only true for weak perturbation of the primary magnetic field.

A particular issue is the choice of the regularization parameter. In our setup we optimize λ so as to meet the Morozov criterion [3]. This criterion states that the optimal value is the one where the variance of the residuals equals the variance of the noise **n**, i. e.

$$\lambda^{opt} = \arg\min_{\lambda} \left(\mathrm{var}(\Psi(\boldsymbol{\kappa}_{reconstr}(\lambda)) - \mathbf{y}_{\mathbf{m}}) - \mathrm{var}(\mathbf{n}) \right) \quad (7)$$

The feasibility of this method was tested in simulations with the following modeling setup:

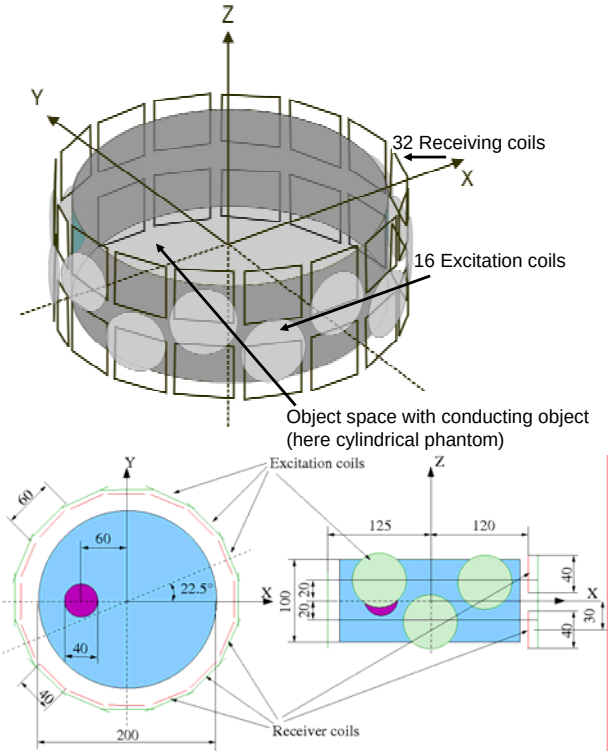

Figure 1: Modeling setup, all measures in [mm]

The object under investigation was a cylindrical conductor (radius and height=100 mm, κ=0.2 S/m) with a spherical inhomogeneity (radius 20 mm) centered at (x=-60, y=0, z=0) [mm] and an array of 16 circular excitation coils (radius 30mm) and 32 receiving coils. The quadratic receiver coils (edge length 40 mm) were placed on two symmetrically arranged parallel rings with a radius of 120 mm, each comprising 16 evenly spaced coils. Adjacing coils in the upper and lower ring were combined in counter-phase so as to simulate 16 planar gradiometers which correspond to those in a true measurement setup which is presented in a complementary paper [5]. The excitation coils were placed in groups of 8 with their centers on two rings with radii of 125 mm in two transversal planes of the cylinder. The centers of the excitation coils were placed in integer multiples of 22.5° and alternating between upper and lower ring. This pattern was chosen in order to avoid a very high symmetry of the excitation patterns which can cause ambiguities in the data [4].

Before any evaluation of eq. 6 the necessary condition of independence of the sensitivity map on frequency was tested. To this end sensitivity maps were generated at 100 kHz and 450 kHz and the mean relative deviation between corresponding voxels was calculated.

Then simulated data **ΔV** were generated with a dedicated reconstruction package. The conductivity of the cylindrical conductor was chosen to be 0.2\,S/m. The conductivity of the perturbation was varied according to a typical spectrum of tissue in the upper ß-dispersion range. This spectrum was calculated with the Cole-model according to

$$\sigma(\omega) = \mathrm{Re}\left\{ \sigma_0 + \frac{\sigma_\infty - \sigma_0}{1 + \left(j \frac{\omega}{\omega_C} \right)^{\alpha}} \right\} \quad (8)$$

with the parameters : σ_0=0.033 S/m, σ_∞=0.373,S/m, ω_C=2π*51006 [rads^{-1}] and α=0.98.

In order to avoid an 'inverse crime' uncorrelated noise was added to the simulated data wereby the standard deviation of the noise voltage was chosen as a percentage of the maximum absolute value occurring in **ΔV.** In this paper 1% noise was added.

Frequency differential images were then reconstructed from the **ΔV** between a reference frequency f_{ref} of 300 kHz and the test frequencies 200, 400 and 700 kHz. The regularization was done with the unit matrix and a regularization parameter λ of 5.1*10^{-18}.

There is one particular difficulty when applying a single-step reconstruction method: The reconstructed values of Δσ are usually much lower than the real ones, i. e. eq. 5 yields the correct search direction but not the correct step size. This is an inherent property of the associated point spread function (psf) and the discrepancy gets worse with increasing regularization, i. e. with increasing noise. Therefore the absolute reconstructed values of Δσ cannot be interpreted quantitatively. However, the ratios of pairs of Δσ at different frequencies are reconstructed correctly, so that it is possible to obtain relative differential conductivity spectra. Let $\Delta\sigma(f_i)$ be the reconstructed conductivity difference between the reference frequency and the frequency f_i. Furthermore let $\Delta\sigma(f_0)$ be the reconstructed conductivity difference between the reference frequency

ISSN: 1727-1983

and an arbitrary base frequency f_0. Then the relative differential spectrum is defined as

$$s(f_i) = \frac{\Delta\sigma(f_i)}{\Delta\sigma(f_0)} \qquad (9)$$

s(f) is dimensionless and has the value 1 at the base frequency f_0. Due to the calculation of a ratio s(f) is independent of the scaling factor caused by the particular psf and thus neither depends on the regularization nor on the location of the perturbation. Moreover s(f) is a shifted and scaled replica of the original conductivity spectrum which does not allow for the extraction of absolute values but which preserves entirely the morphology of the spectrum.

The feasibility of this approach was tested by reconstructing s(f) between 200 and 700 kHz with a f_{ref} =100 kHz and a f_0=200 kHz. The reconstructed s(f) data were compared with the expected values from the true spectra as calculated with eq. (9).

Results

(1) Evaluation of the sensitivity matrix: The mean relative deviation between corresponding entries of the sensitivity matrix at 100 and 450 kHz was no more than 0.0017%, respectively. This suggests that the assumption of pure scaling of this matrix is justified and that the scaling formula (6) is valid.

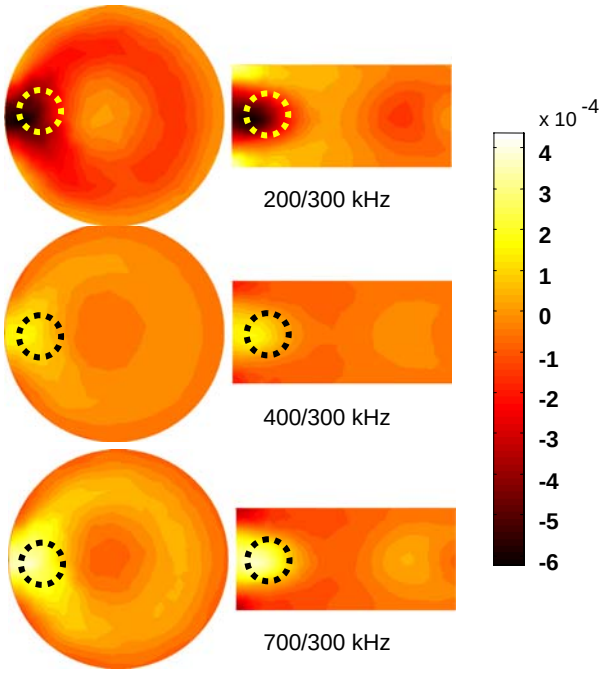

Figure 2: frequency differential images of the perturbed cylinder at three different frequencies. The dotted circles delineate the original position of the perturbation.

(2) frequency differential images: Fig. 2 shows the reconstructed conductivity difference at 100, 300 and 700 kHz with a reference frequency of 200 kHz. Transversal and saggittal cross-section of the cylinder are depiced which contain the center of the perturbation.

The position of the perturbing sphere is localized fairly correctly, however there is a certain outward shift and considerable smearing. The scaling of the data is clearly visible when comparing the reconstructed differences (see colorbar) with the true ones (-0.012 S/m between 200 and 300 kHz and 0.0089 S/m between 700 and 300 kHz). The resulting factor lies in the range of 20.

(3) Reconstruction of a relative differential spectrum.

Table 1 shows the values of the relative differential spectrum s(f) at 5 discrete frequencies. The relative error between reconstructed and expected values remained below 2.5 % in any case. In fig. 3 the corresponding graphical representation of the relative spectra is given.

Table 1: relative differential spectrum s(f)

frequency	**true value**	**reconstructed value**	**Relative error**
kHz	S/m	S/m	
300	1.24	1.217	-1.89
400	1.332	1.309	-1.72
450	1.358	1.330	-2.09
600	1.402	1.377	-1.75
700	1.418	1.386	-2.23

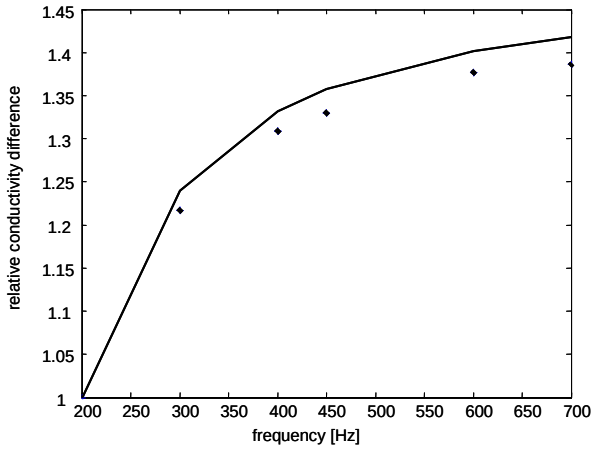

Figure 3: Graphical representation of the relative differential spectrum listed in table 1. The solid line delineates the expected values, the dots are the reconstructed values.

Discussion

The shown analysis demonstrates the theoretical feasibility of differential MIT spectroscopy with a single-step reconstructor. The obtained values deviate from the true ones by less than 2.5%. The reconstructed

ISSN: 1727-1983

values remain below the expected ones, whereby the discrepancy increases slightly with the frequency. This is probably due to the fact that a single-step reconstructor relies on the assumption of a linear mapping, which is not the case in MIT. In fact the non-linear effects increase with increasing conductivity difference, i. e. with increasing frequency difference. The images shown in fig. 2 clearly show the change of the contrast with the frequency, whereby the perturbation appears negative in the first image, where the measurement frequency is lower than the reference frequency. At all frequencies higher than the reference frequency the contrast becomes positive and increases with the frequency, as is expected from the Cole-spectrum. The image of the sphere is smeared out due to the regularization procedure and shifted towards the border. Both effects are inherent in the point spread function of MIT when using the unit matrix for regularization. The ring-shaped artefact in the top view at a radius of about 60% of the cylinder radius is some kind of a ringing artefact which is also typical for the particular psf and may be mitigated by more advanced regularization and filtering techniques.

Fig 4 demonstrates the feasibility of the reconstruction of relative differential spectra from MIT data. The successful experimental validation of this method is shown in a complementary paper in this issue [5]. Further research will be dedicated to the improvement of the reconstruction algorithms and to the identification of physiological parameters by fitting appropriate tissue models (e. g. The Cole model) to the reconstructed spectra.

Conclusion

Multifrequency MIT appears as a promising approach to generating low-resolution images of physiological processes which are associated with the frequency dependence of the electrical conductivity. Examples are: Tissue discrimination, hydration monitoring, ischemic events, detection of hemorrhages. The image quality is comparable to that of electrical impedance tomography. The particular advantage of MIT is the contact-less operation and the possibility to overcome electrical barriers such as the skull in brain imaging.

References:

[1] Brunner, P., Merwa, R., Rosell, J., Scharfetter, H. (2005): 'Reconstruction of the shape of conductivity spectra using differential multi-frequency MIT', Proc. 6th Conference on Biomedical Applications of Electrical Impedance Tomography, London

[2] Griffiths, H. (2001): 'Magnetic induction tomography', Meas. Sci. Technol., 26, pp. 1126-1131

[3] Hansen, P.C. (1998): 'Rank-deficient and discrete ill-posed problems', SIAM, Philadelphia

[4] Merwa, R., Hollaus, K., Brunner, P., Scharfetter, H. (2005): 'Solution of the inverse problem of magnetic induction tomography (MIT)'. Physiol. Meas., 26, pp. S241–S250

[5] Missner, A., Merwa, R., Brunner, P., Scharfetter, H. 'Magnetic induction tomography spectroscopy of living tissues: experimental validation', this issue

[6] Scharfetter, H., Casañas, R., Rosell, J. (2003) 'Biological tissue characterization by magnetic induction spectroscopy (MIS): requirements and limitations', IEEE Trans. Biomed. Eng., 50: pp. 870-880

ISSN: 1727-1983